Techniques and Experimental Results for Performance Analysis of Photovoltaic Modules Installed in Buildings

Available online at www.sciencedirect.com

ScienceDirect

Energy Procedia 111 (2017) 944 – 953

Energy Procedia

8th International Conference on Sustainability in Energy and Buildings, SEB-16, 11-13 September 2016, Turin, ITALY

Techniques and Experimental Results for Performance Analysis of Photovoltaic Modules Installed in Buildings

F. Spertino [a]*, J. Ahmad [a], A. Ciocia[a], P. Di Leo[a]

[a]*Politecnico di Torino, Energy Department, corso Duca degli Abruzzi, 24 – 10129 Torino, Italy*

Abstract

Photovotaic (PV) modules applied to buildings form a unique surface at the same roof inclination, replacing the tiles. Such PV systems are affected by thermal and mechanical stresses, and remarkable dirt. Another issue is the partial shading with possible failure of bypass diodes. In this paper a sample of PV modules, affected by the previous issues, was tested by electroluminescence and I-V curve scanning, to quantify power losses according to the causes. The experimental results are presented, demonstrating that the most important causes of losses are the cracks in module's solar cells and the failure of their bypass diodes.

Peer-review under responsibility of KES International.

Keywords: PV module; experimental techniques; electroluminescence; *I-V* curve scanning; building applied PV.

1. Introduction

It is very advisable the installation of Photovoltaic (PV) generators in urban areas to create distributed generation, which permits to produce a substantial amount of the electricity close to the demand [1]. However, some technical issues arise when conventional PV modules are attached in building rooftop subjected to aesthetical and economic constraints. These constraints may be summarized in three items studied in this paper. Firstly, the installation of PV modules must be at the same height of the roof tiles, replacing them. Secondly, the PV modules must have the same tilt angle of the roof. Thirdly, the PV modules must be placed close each other to form a unique surface, even in the presence of obstacles on the roof, to minimize the usage of metallic structures and the time of installation. The linked

* Corresponding author. Tel.: +39-011-0907120.
E-mail address: filippo.spertino@polito.it

Peer-review under responsibility of KES International.
doi:10.1016/j.egypro.2017.03.257

technical issues, described in this paper, generate a worsening of the operational performance up to the complete failure of PV modules. To detect this underperformance, appropriate techniques are employed to quantify the amount of power losses and to recognize their causes.

As well known, the PV modules are subject to many experimental tests before their operational life. They are the qualification tests to simulate 25 years of exposition to the environmental agents. The degradation rate of PV modules is artificially accelerated within a few days of tests in laboratory. On the other hand, the techniques to determine the performance of PV modules, during their life, regard both the electrical efficiency and the structural adequacy of the solar cells inside every PV module. These techniques include the measurement of the current-voltage (*I-V*) characteristic curves and the evaluation of images from thermo-graphic cameras with different wavelength bands. Such bands are 7.5—13 μm for hot spot identification and 1.1—1.2 μm for electroluminescence. The abovementioned tests may be periodically performed to check if the PV system behavior is satisfying. The test for hot spot identification is normally performed in field with the PV modules in operation to detect hot cells when, in shading conditions, good cells supply power to defective cells. The electroluminescence test carried out in dark room, after disassembly of a PV module from metallic structure, provides qualitative information about the electrical efficiency of the solar cells inside the PV module under test. The color uniformity of the cells and their brightness are a qualitative warranty of good efficiency. On the other hand, to have available an adequate amount of information, it is needed to carry out the Laser Beam Induced Current (LBIC) test [2]; however, this is a very expensive test. Usually, the electroluminescence test, together with the information provided by the correction of the I-V curve measurement to STC, is sufficient to determine the behavior of a PV module and the possible causes of its underperformance. Further tests, to be performed in case of evident reduction in the open circuit voltage, regard the measurement of the *I-V* curves of bypass diodes. They are connected in anti-parallel to groups of solar cells inside the junction box of the PV module to protect the cells against the generation of reverse voltage as a consequence of I-V mismatch for shading effect.

This article provides a deep understanding of the amount and causes of performance worsening. The experimental tests are carried out in outdoor conditions if they regard the *I-V* curves and in laboratory if they concern the electroluminescence.

Nomenclature

α_T	temperature coefficient of short circuit current (A/°C)
β_T	temperature coefficient of the open circuit voltage (V/°C)
FF	fill factor of the *I-V* curve, corresponding to ratio $P_{max}/(V_{oc} \cdot I_{sc})$
G	solar irradiance (W/m^2), at standard test conditions G_{STC}=1000 W/m^2
η	PV conversion efficiency
$I_{mpp,c}$	current in maximum power point, corrected to standard test conditions (A)
$I_{mpp,d}$	current in maximum power point at STC, declared by manufacturer (A) — $\Delta I_{mpp,rel} = (I_{mpp,c} - I_{mpp,d})/I_{mpp,d}$
I_{Pmax}	current in maximum power point measures at experimental conditions (A)
$I_{sc,d}$	short-circuit current at STC declared by manufacturer (A)
I_{sc}	short-circuit current measured at experimental conditions (A)
N_s	number of series connected cells
$P_{mpp,c}$	maximum power corrected to STC (W)
$P_{mpp,d}$	maximum power at STC declared by manufacturer (W) — $\Delta P_{rel} = (P_{mpp,c} - P_{mpp,d})/P_{mpp,d}$
P_{max}	maximum power measured at experimental conditions (W)
T_a	ambient temperature (°C)
T_C	cell temperature T_C (°C), at standard test conditions T_{STC}= 25°C
$V_{mpp,c}$	voltage in maximum power corrected to STC (V)
$V_{mpp,d}$	voltage in maximum power point at STC declared by manufacturer (V) — $\Delta V_{mpp,rel} = (V_{mpp,c} - V_{mpp,d})/V_{mpp,d}$
V_{Pmax}	voltage in maximum power point measured at experimental conditions (V)
$V_{oc,d}$	open circuit voltage at STC declared by manufacturer (V)

2. Aesthetical and economic constraints to the PV module installation on rooftop

As written in Introduction section, conventional PV modules applied to buildings (well-known as BAPV) may be affected by many technical issues, as a result of aesthetical and economic constraints. These constraints and the consequent issues are summarized in the following.

- It is necessary to install the conventional PV modules above a waterproof and thermally insulated layer, because they are not waterproof, if placed close each other at the same height of the roof tiles. This type of installation (called in Italy "totally integrated" Fig 1a) exhibits, thus, *poor ventilation*. Furthermore, the tiles may carry dirty rain and dust on the PV modules, if the tiles are at a higher level than the PV modules (Fig. 1a). This implies a *major impact of dirt* with respect to the installation above the tiles thanks to metallic structures with brackets (Fig. 1b called in Italy "partially integrated").
- PV modules, installed with the same inclination of the roof, normally have tilt angles <25° and they receive in summer daily global irradiations higher than those achieved with optimal inclination angles (e.g., ≈30° in Southern Italy and ≈40° in Northern Italy) from the viewpoint of the yearly irradiation. In turn, higher irradiation means *higher cell temperature just in summer* when the ambient temperature reaches its peak. This effect is superimposed on the issue described in the first item of this list.
- The surface covered by the PV modules must be unique. Actually, regular geometries are considered the best solution to obtain a good aesthetical result, minimize the usage of metallic structure and reduce the time of installation. Nevertheless, if the installers do not leave enough space to walk (walkways around modules), they may walk on the PV modules during maintenance. The result may be a *mechanical damage* of the PV cells with hot spot formation and huge underperformance.
- Sometimes obstacles are present on the roof or near it: they may be chimneys, antennas, poles and masts. They can create *partial shading* on the PV array during the day. Continuous shadowing is source of both hot spots in the PV cells and long operation of bypass diodes. In Fig. 1c, an antenna creates partial shading on two of the 15 PV modules regularly placed to form a rectangle (left side). A solution is the installation of fewer modules with higher efficiency (e.g., heterojunction of monocrystalline and amorphous silicon) [3], as shown in the right side of the same figure.

Table 1. Electrical Rated Parameters (at STC).

	group #1	**group #2**
$P_{mpp,d}$	228 W	300 W
Tolerance ($P_{mpp,d}$)	±3%	±3%
$V_{oc,d}$	36.2 V	47.05 V
$V_{mpp,d}$	29.93 V	37.98 V
$I_{sc,d}$	8.16 A	8.40 A
$I_{mpp,d}$	7.65 A	7.90 A
N_s	60	72
η	14.2	15.3

In order to quantify the worsening issues up to the complete failure for the abovementioned constraints, the authors selected 16 PV modules from totally integrated PV systems installed between 2011 and 2013 on residential and commercial buildings in Northern Italy. As a comparison to check the presence of possible production defects, 3 new PV modules of the same manufacturer were tested before the sunlight exposure. The aged PV modules were divided in two groups. In group #1, 10 PV modules were selected for the presence of snail-tracks, extreme dirt and bird droppings. In group #2, 6 PV modules were characterized by partial shading and defects in V_{oc} and I_{sc}. The main rated parameters at STC of the two groups of polycrystalline Si modules are shown in Table 1.

(a) (b)

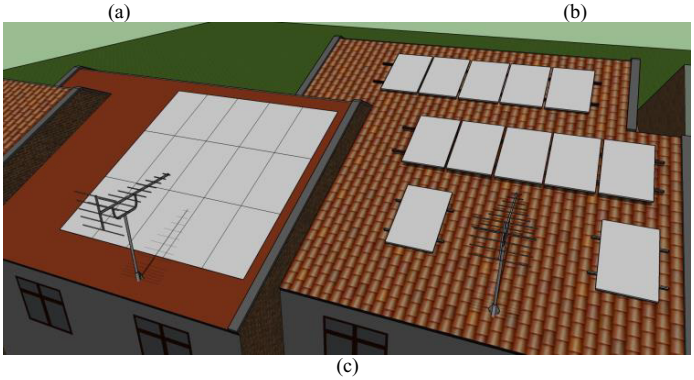

(c)

Fig. 1. PV modules on rooftop in "totally integrated" version (a), in "partially integrated" version (b) and their comparison (c).

3. Techniques for performance analysis and detection of defects

3.1. Tracing the I-V curve by capacitor method

The measurement of the I-V characteristic of a PV module is a necessary tool to estimate its performance. The authors adopted the capacitive-load based technique, in which voltage, current, irradiance and temperature were measured at the same time [4]. The experiment started with the closing of the power breaker (Fig. 2): the capacitor was charged from short circuit to open circuit condition and signals were simultaneously measured. After the end of the experiment, the capacitor was disconnected by the PV generator opening the breaker and data were stored for post-processing. Before the next measurement, the capacitor was discharged by a resistance.

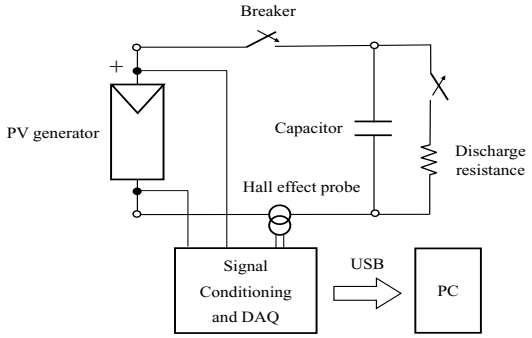

Fig. 2. Measurement scheme for the current-voltage characteristic of a PV array.

The Automatic Data Acquisition System (ADAS), used here for the characterization of the *I-V* curve measurement, was composed of:

- # 1 personal computer;
- # 1 multifunction data acquisition device, equipped with A/D converter, successive approximation, 16 bit-resolution with maximum sampling rate of 1.25 MSa/s;
- # 1 voltage differential probes, attenuation ratios 20:1, 200:1, range ±1000 Vpk;
- # 1 current probe (Hall effect), 30 A_{pk} for DC/AC;
- # 1 secondary standard pyranometer and #1 irradiance sensor in poly-crystalline silicon (p-Si);
- # 1 thermometer (thermistor) for ambient temperature.

The *I-V* curve test was carried out in a short time (maximum duration ≤100 ms) in order to keep constant irradiance and temperature [5]. However, as written in [6], to minimize the effect of parasitic parameters, the *I-V* curve must be traced slowly (the total capacitor charging time >20 ms). According to these constraints and the PV module specifications, the appropriate capacitance was 5 mF. After the measurements, correction method in [7] was used to correct data to Standard Test Conditions. Another standard taken into account for the correction was [8]. The temperature coefficients of short circuit current α_T and of the open circuit voltage β_T, supplied by the PV modules' manufacturer, were used. The relative difference of power ΔP_{rel}, voltage $\Delta V_{mpp,rel}$ and current $\Delta I_{mpp,rel}$ were calculated by comparing measured values and rated values provided by the modules' manufacturer.

The most important physical quantities taken into account and the corresponding measurement uncertainties are clarified below:

- for the solar irradiance G the absolute uncertainty is of ±20 W/m^2, for the ambient temperature T_a the absolute uncertainty is of ±0.2 °C, for the cell temperature T_C the absolute uncertainty is of ±2 °C;
- I_{sc} is the short-circuit current and V_{oc} is the open circuit voltage of the PV generator (with uncertainties of ±1% and ±0.1%, respectively);
- for the fill factor FF uncertainty is ± 2 %;
- $P_{mpp,c} = V_{mpp,c} \cdot I_{mpp,c}$(STC) is the maximum power of the generator at STC (with measurement uncertainty of ± 4 %).

3.2. Electroluminescence tests in dark room

Electroluminescence (EL) is a non-destructive testing technique that permits to identify defects with high resolution. A totally shaded PV generator emits radiation (like a light emitting diode), that can be detected by a sensitive camera. Crystalline silicon PV cells emit in the infrared region of the spectrum: the signal is within 950—1350 nm and the peak, corresponding to the bandgap, is ≈1150 nm [9]. The sensitive camera may be a silicon charge-coupled device (CCD). In the EL test the PV generator is placed in a dark room and supplied with an external excitation current (lower than I_{sc}). The filtered camera takes an image and then it is processed.

The result is an image characterized by defective portion of solar cells (isolated or not properly working areas) looking darker than perfectly working cells. In order to optimize the quality of the image and properly detect different kind of defects, the external excitation current is changed and the experiment is repeated. According to [10], low excitation currents permit to identify defects in materials, while higher currents are used to detect problems in electrical contacts. The tests were performed in dark room, in order to avoid noise due to other infrared sources and reflections. EL test images were used to identify defects and also to understand their causes (e.g., defective production processes, not carefully transport and installation). The hardware, used by the authors to perform EL tests, was composed of a power supply with 35—70 V_{DC} e 5—10 A_{DC} and a photo-camera with CCD sensor (6.10 Mpixel) and infrared filter (800 nm).

4. Experimental results

The rated power of the 10 PV modules in group #1 was $P_{mpp,d}$=228 Wp ±3% and they have been made up with N_s=60 series cells (size of a single cell = 156 x 156 mm). Every module included 3 bypass diodes, each protecting a string of 20 cells. The 6 PV modules in group #2 had higher rated power ($P_{mpp,d}$=300 W_p) and higher number of cells (N_s=72), with respect to group #1. In this case the 3 bypass diodes protected a string of 24 cells.

a) b) c)

Fig. 3. Group #1: PV modules affected by extreme dirt (a) (b) and bird droppings (c).

4.1. Dirt on glass surface and cell cracks

The PV modules in group #1 were uninstalled from totally integrated plants without walkways. They were selected in order to check underperformance related to:

- extreme dirt on all the surface of the modules with high concentration close to the edge of the metallic frame (Fig. 3a and 3b) and many bird droppings (Fig. 3c);
- possible mechanical damage (shoe footprints were detected on the glass surface during inspection);
- snail tracks on many solar cells.

Regarding the dirt impact, the *I-V* scan was performed before and after cleaning. The measurement of the *I-V* curves and correction to STC have highlighted that the maximum power $P_{mpp,c}$ of dirt modules were much lower than the declared values $P_{mpp,d}$. The values of ΔP_{rel} ranged from -31% to -53%, corresponding to $P_{mpp,c}$ values between 107 and 157 W. After cleaning, ΔP_{rel} decreased and ranged from -21% to -48%, corresponding to $P_{mpp,c}$ values between 118 and 180 W. As in [11] and [12], losses due to dirt sometimes can be ≥4%: in this case, they ranged from -4% to -10% and the average was ≈7%.

The classical one diode model of a PV cell [13] includes current source I_{ph}, a single exponential diode I_j and shunt resistance R_{sh} all connected in parallel and a resistance in series R_s. The single exponential diode I_j is modelled by two parameters: the ideality factor n and the dark saturation current I_0. I_{ph} represents the photo-generated current according to solar spectrum and spectral response. The shunt resistance R_{sh} takes into account leakage current I_{sh}. flowing through lateral surfaces and grain boundary in polycrystalline silicon. The series resistance R_s represents the current flow through the emitter and base of the solar cell and contact resistances. If the voltage across the diode is U_j, the voltage U between the load terminals and its absorbed current I can be defined by (1) and (2), respectively:

$$I = I_{ph} - I_0 \cdot \left(e^{\frac{q \cdot U_j}{n \cdot k \cdot T}} - 1 \right) - \frac{U_j}{R_{sh}} \tag{1}$$

$$U = U_j - R_s \cdot I \tag{2}$$

where q (C) is the electron charge, k (J/K) is the Boltzmann constant and T (K) is the cell temperature.

As written before, the modules were affected by snail-tracks and showed high underperformances, also after cleaning. The results of three tests on one of the PV modules are presented in Table 2: the maximum power was more than halved. The power loss is totally due to the high reduction of current: it decreased from 7.65 A (declared by manufacturer) down to ≈3.54 A (measured at STC), corresponding to a deviation ΔI_{mpp}≈-53%. In Fig. 4 the *I-V* curve of test #2 is compared with the *I-V* curve at STC declared by manufacturer. Experiments are performed at irradiance $G \approx G_{STC}$ and at cell temperature (T_c=52°C) higher than T_{STC}. For this reason the open circuit voltage (V_{oc}=32.82 V) of the defective module was lower than the declared value ($V_{oc,d}$=36.2 V). The main issues in the *I-V* characteristic were the following:

- current I_{ph} was strongly reduced for each string of cells with #3 as the worst string;
- the lowest current (string #3) caused discontinuity in the slope of the *I-V* curve, corresponding to the voltage of two 20-cell strings as a consequence of the bypass diode conduction;
- slope of the *I-V* curve near I_{sc} higher than the normal slope, corresponding to a decreased R_{sh} value;
- slope of the *I-V* curve near V_{oc} lower than the normal slope, corresponding to an increased R_s value.

Table 2. Experimental results on a PV module of the group #1.

Experimental conditions	Test #1	Test #2	Test #3	Average	
T_a	21	22	21	21	°C
G	1004	976	981	987	W/m^2
T_c	52	52	52	52	°C
P_{max}	98	95	95	96	W
V_{Pmax}	27.38	27.01	26.85	27.08	V
V_{oc}	32.81	32.82	32.85	32.83	V
I_{Pmax}	3.56	3.51	3.55	3.54	A
I_{sc}	5.61	5.59	5.68	5.63	A
FF	52.9%	51.7%	51.1%	51.9%	
Parameters at STC					
P_{mpp}	106	108	108	107	W
V_{mpp}	31.22	29.52	3.23	30.32	V
I_{mpp}	3.40	3.65	3.56	3.54	A
Other parameters					
ΔP_{rel}	-53.5%	-52.7%	-52.8%	-53.0%	
$\Delta I_{mpp,rel}$	-55.6%	-52.3%	-53.4%	-53.8%	
$\Delta V_{mpp,rel}$	4.3%	-1.4%	1.0%	1.3%	
η	6.6%	6.7%	6.7%	6.7%	

In order to check the presence of mechanical defects in solar cells, the electroluminescence test was performed. The results demonstrated a high number of cracks and isolated portions of cells in each module: these defects were observed mainly along snail-tracks, which affect at least 24 cells in the least damaged module up to all the cells in the worst one. The image, related to one of the analysed modules (Fig. 5), is representative of the whole group of 10 modules: broken cells were many and randomly distributed. Generally, a uniform distribution of cracks occurs when a heavy distributed load (like snow) is on the whole front of the module [14]. The abovementioned presence of shoe footprints on the glass surface, the absence of broken cells in new modules and the random distribution of cracks confirmed that they were stepped on during maintenance (or installation). The electroluminescence indicated the presence of cracks and inactive parts of cells. When a cell is broken, parts of it can be disconnected from the circuit and becomes inactive. The result, in the equivalent circuit, is a decreased current I_{ph}, proportional to the active area.

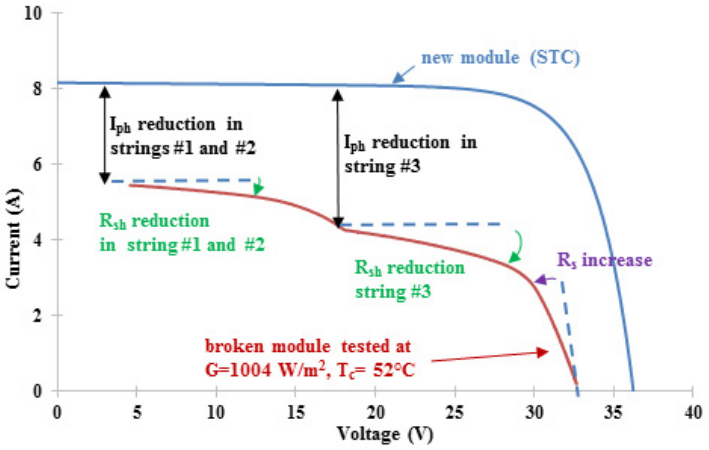

Fig. 4. Comparison between the *I-V* curves of a new module at STC and a broken module during test.

As written in [15], cracks are localized in the emitter region of the solar cells and act as a shunt. They can be modelled as additional low parallel resistances inside the cells (called volume shunts) between the sides of the p-n junction. The creation of further paths for the leakage current is modelled with a decreased R_{sh} value. The partial disconnection of a busbar provokes a dark colour in the portion of the cell where the busbar collects the photovoltaic current, while the other portion of the cell appears more bright than a normal cell. The result is an increment of R_s.

4.2. Failures in bypass diodes due to thermal stress

As written in Section II, poor ventilation and partial shading cause overheating of the PV modules. In case of partial shading, bypass diodes work to protect cells and reduce power losses. Under normal operation, the solar cells are forward biased: bypass diodes are reversed biased and they can be considered as an open circuit. If one cell is shaded, it conducts less current with respect to unshaded cells. In this case, if the current required by load is high, the bypass diode becomes forward biased and conducts. An amount of current from the unshaded cells flows in the diode and only the group with the shaded cell results not productive. The consequences of partial shading are the shaded cell working as a load and the conduction of the bypass diode. The result is the increment of the internal temperature of both shaded cell and bypass diode.

To assess the appropriateness of the thermal design (too hot temperatures damage the p-n junctions) and the long-term reliability of bypass diodes used inside the PV modules, a thermal qualification test is required by [16]. This test is defined as “bypass diode thermal test”. Initially, the temperature inside the junction box is 75 °C, then the bypass diodes become conductive with a specified current for a specified duration.

After the thermal test, the bypass diodes must operate correctly. Nevertheless, this test is performed to check diodes working for few hours per day, because shadows generally should not occur during the whole day and diodes should not work for too many hours. If a poor air circulation with high working temperatures (70-75° C) occurs (e.g., due to total integration), thermal stress increases and accelerate the damage process.

During the inspection, the modules in group #2 exhibited negligible open circuit voltage and short circuit current, while the junction-box covers were extremely hot. After removal of the junction-box covers, most of the bypass diodes had changed their original black colour into an opaque brown colour. Thus, all the bypass diodes were disconnected. They were supplied by a regulated power supply and some points of the *I-V* curve were measured. Most of the diodes revealed irreversible short circuit failure: at least two diodes per each module were broken. As shown in Fig. 6, the *I-V* curves of broken diodes affected by overheating corresponded to low resistances (≈400 mΩ) in both the quadrants. The typical unidirectional behaviour of a diode was no longer verified.

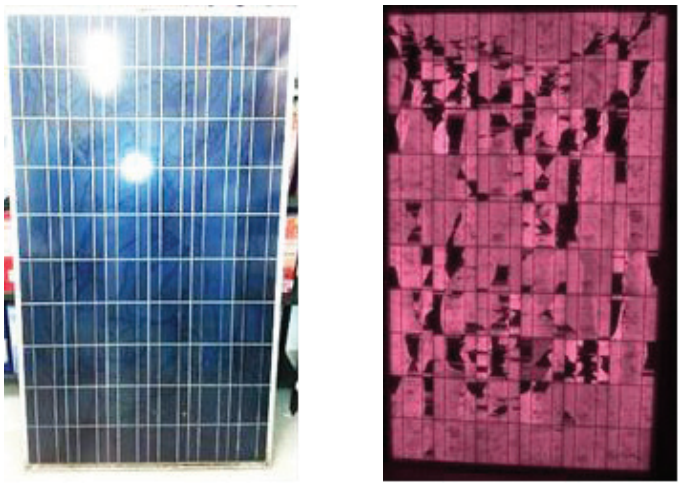

Fig. 5. Photo and electroluminescence image of a PV module of the group #1.

The measurements of the *I-V* curves of modules without bypass diodes, their correction to STC and the electroluminescence test highlighted that:

- PV modules with 300 W_p exhibited maximum powers at STC within the declared values;
- electroluminescence test clarified the absence of cracks (except that in one/two cells per PV module).

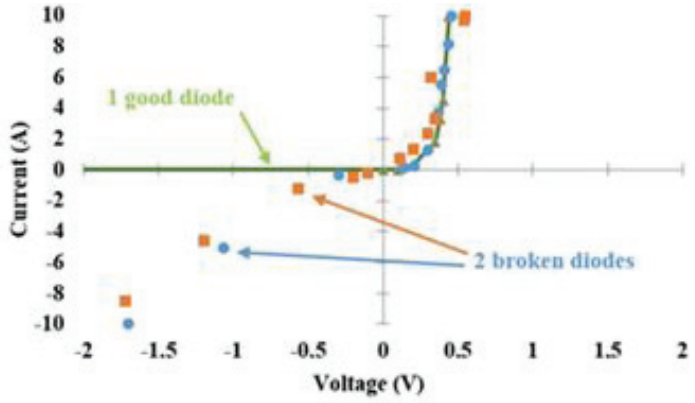

Fig. 6. Result of I-V test on three diodes: 1 well working and 2 affected by overheating.

5. Conclusions

As a result of preliminary study of underperformance, two groups of PV modules on rooftops were identified. The first group was selected from PV systems affected by the presence of snail-tracks, extreme dirt and bird droppings. The scanning of the *I-V* curve was performed before and after cleaning and results were compared. By itself, the dirt caused in average power losses 7% with a peak of ≈10%. After cleaning, power losses due to other causes ranged from 21% to 48%. The results of electroluminescence demonstrated a high number of cracks randomly distributed and isolated portions of cells where the snail-tracks were present. The cause was: PV systems installed without walkways and workers' stepping on them during maintenance. The consequent power losses advise the replacement of the PV modules.

The second group of tested modules were selected from PV systems affected by partial shading and poor ventilation. During the inspection, the PV modules exhibited negligible open circuit voltage and short circuit current. Moreover, the junction-box covers were extremely hot. After removal of junction-box covers, it was observed that many bypass diodes had changed their original appearance. The *I-V* curves of all the diodes were scanned: most of them revealed irreversible short circuit fault. On the contrary, the *I-V* scanning of PV modules without diodes exhibited maximum powers within the declared values at STC and the EL tests clarified the absence of cracks. In this case, the simultaneous presence of partial shading and poor ventilation, for the PV modules applied to the rooftops, provoked the fault of bypass diodes. After diode replacement, the PV modules can return to work.

References

[1] Jamil M, Anees AS, Optimal sizing and location of SPV (solar photovoltaic) based MLDG (multiple location distributed generator) in distribution system for loss reduction, voltage profile improvement with economic benefits, Energy 2016, 231:39-103.
[2] Padilla M, Michl B, Thaidigsmann B, Warta W, Schubert MC, Short-circuit current density mapping for solar cells, Solar Energy Materials and Solar Cells 2014, 282:88-120A.
[3] Spertino F, Corona F, “Monitoring and checking of performance in photovoltaic plants: A tool for design, installation and maintenance of grid-connected systems”, Renewable Energy 2013, 722:32-60.
[4] Attivissimo F, Adamo F, Carullo A, Lanzolla AML, Spertino F, Vallan A, ”On the performance of the double diode model estimating the maximum power point for different photovoltaic technologies”, Measurement 2013, 3549:59-46.
[5] Adamo F, Attivissimo F, Di Nisio A, Spadavecchia M, ”Characterization and testing of a tool for photovoltaic panel modeling”, IEEE Trans. Instr. Meas. 2011, 1613:22-60.
[6] Spertino F, Ahmad J, Ciocia A, Di Leo P, Murtaza AF, Chiaberge M, ”Capacitor charging method for *I-V* curve tracer and MPPT in photovoltaic systems,” Solar Energy 2015, 461:73-119.
[7] IEC 60891:2009-12, Photovoltaic devices - Procedures for temperature and irradiance corrections to measured *I-V* characteristics.
[8] EN 60904-5:2011 “Photovoltaic devices - Part 5: Determination of the equivalent cell temperature (ECT) of the photovoltaic (PV) devices through the open circuit voltage method”.
[9] Fuyuki T, Hayato K, Tsutomu Y, Takahashi Y, Yukiharu U, ”Photographic surveying of minority carrier diffusion length in polycrystalline silicon solar cells by electroluminescence”, Applied Physics Letters 2005, 461:73-86.
[10] Ebner R, Kubicek B, Ujvari G, ”Non-destructive techniques for quality control of PV modules: infrared thermography, electro- and photoluminescence imaging”, Industrial Electronics Society - 39th Annual Conference of the IEEE; 2013. p. 8104-8109.
[11] Spertino F, Ciocia A, Di Leo P, Tommasini R, Berardone I, Corrado M, Infuso A, Paggi M, A power and energy procedure in operating photovoltaic systems to quantify the losses according to the causes, Solar Energy 2015, 313:26-118.
[12] Tanesab J, Parlevliet D, Whale J, Urmee T, Pryor T, The contribution of dust to performance degradation of PV modules in a temperate climate zone, Solar Energy 2015, 147:57-120.
[13] Spertino F, Sumaili J, Andrei H, Chicco G, "PV module parameter characterization from the transient charge of an external capacitor," IEEE Journal of Photovoltaics 2013, 1325:33-3.
[14] International Energy Agency, Performance and Reliability of Photovoltaic Systems, Review of Failures of Photovoltaic Modules, Report IEA-PVPS Task 13, 2014.
[15] El Amrani A, Mahrane A, Moussa FY, Boukennous Y, El Kechai A, Experimental optimization of solar cells edge junction passivation, Materials Science in Semiconductor Processing 2013, 51:57-16.
[16] IEC 61215:2005, Crystalline Silicon Terrestrial Photovoltaic (PV) Modules - Design and Type Approval, International Electrotechnical Commission, Second edition.